Available online at www.sciencedirect.com
SCIENCE DIRECT®
Carbohydrate Research 338 (2003) 95–107
CARBOHYDRATE RESEARCH
www.elsevier.com/locate/carres

Depicting the MM3 potential energy surfaces of trisaccharides by single contour maps: application to β-cellotriose and α-maltotriose

Carlos A. Stortz,* Alberto S. Cerezo

Departamento de Química Orgánica-CIHIDECAR, Facultad de Ciencias Exactas y Naturales, Universidad de Buenos Aires, Ciudad Universitaria, 1428 Buenos Aires, Argentina

Received 30 July 2002; accepted 16 September 2002

Abstract

The adiabatic potential energy surfaces (PES) of two trisaccharides (β-cellotriose and α-maltotriose) were obtained using the MM3 force field. Each PES can be described by a single 3D contour map for which the energy is plotted against the two ψ glycosidic angles. Given the usually small variations of the ϕ glycosidic torsional angle in the low-energy regions of disaccharide maps (at least with MM3), it is valid to leave both ϕ glycosidic angles to relax in the process of building the conformational map of trisaccharides. The surfaces are those expected from the map of disaccharides containing the same linkages and monosaccharide units (i.e., β-cellobiose and α-maltose), with second-order factors altering the 'symmetry' of both linkages. A large low-energy region appears for β-cellotriose, comprising four minima in close proximity, with barriers between them below 0.6 kcal/mol. On the other hand, for α-maltotriose a main global minimum is observed, with several surrounding local minima. The surfaces obtained agree with single-crystal X-ray data on these trisaccharides and derivatives. A reduction of the linkage flexibilities is observed when passing from the disaccharides to the trisaccharides. Furthermore, the linkage closer to the reducing end appears to be less flexible than the linkage closer to the non-reducing end.

Keywords: Trisaccharides; Conformational analysis; Molecular mechanics; MM3; Ramachandran map; Potential energy surfaces

1. Introduction

Conformational analysis of disaccharides is usually accompanied by the generation of a Ramachandran-like 3D contour map as a tool in understanding their conformational features.[1–3] In these maps the energy is determined for all mutual orientations of the monosaccharide residues, expressed by the glycosidic angles ϕ and ψ. Maltose and cellobiose received the most attention, as typical structures of disaccharides that might be extrapolated to polysaccharides. The early rigid residue analysis was replaced by flexible residue analysis by the pioneering work of Melberg and Rasmussen.[4,5] After the introductory work of Tvaroška and Pérez,[6] the relaxed energy maps of maltose and cellobiose were fully described.[7–10] With the appearance of the MM3 force-field, which is considered very reliable for carbohydrates, the maps for those disaccharides were obtained,[2,11–13] and the methodology to acquire the maps was established. Several attempts to correlate the calculated structures for maltose and cellobiose with experimental parameters in solution, like optical rotations and NOE calculations have been carried out.[14–19] More recently, DFT/ab initio calculations were carried out for maltose,[20] and the AMBER force-field parameters were modified to reproduce those results.[21]

In the several extrapolations to higher oligosaccharides that have been made,[22–26] usually each glycosidic linkage was taken independently, giving rise to one ϕ, ψ contour map per glycosidic linkage. We have recently shown[27] that, as usually the ϕ glycosidic angle takes a more or less fixed value (at least with MM3), it can be added to the variables to relax, and thus, a clear correlation is found for the contour maps with the energy related to ϕ and ψ, and to x–y plots with the energy just related to ψ.[27] Herein we present the possibility of extending those plots for disaccharides relating E versus ψ to depict the potential energy surfaces of

* Corresponding author. Tel./fax: +54-11-45763346
E-mail address: stortz@qo.fcen.uba.ar (C.A. Stortz).

0008-6215/03/$ - see front matter
PII: S0008-6215(02)00360-9

trisaccharides in the way of a contour map in which the energy is plotted as a function of both ψ glycosidic angles. The method is herein applied to the most typical homologous trisaccharides, i.e., cellotriose (β anomer) and maltotriose (α anomer). Although we are showing the results obtained using MM3, this procedure can be used with any potential energy function which leaves the ϕ angle more or less fixed in the low-energy regions.

2. Methods

The molecular mechanics program MM3(92) (QCPE, Indiana University, USA), developed by Allinger and co-workers, was used,[28,29] but the MM3 routines were modified as suggested[30] by changing the maximum atomic movement from 0.25 to 0.10 Å. A dielectric constant of 4.0 was used throughout all the work in order to compare with published data.[11,12] Minimization was carried out by the block diagonal Newton–Raphson procedure for grid points and using the full-matrix procedure for minima. The dihedrals ϕ and ψ for maltose and cellobiose are defined by atoms O-5′–C-1′–O-1′–C-4 and C-5–C-4–O-1′–C-1′, respectively, while ϕ^{H} and ψ^{H} are defined by atoms H-1′–C-1′–O-1′–C-4 and H-4–C-4–O-1′–C-1′, respectively. For maltotriose and cellotriose, the monosaccharides that make up the trisaccharides are numbered starting from the reducing end, and the glycosidic torsional angles are named as follows:

$\phi_{2\rightarrow1}$ defined by atoms O-5′–C-1′–O-1′–C-4, $\psi_{2\rightarrow1}$, by atoms C-5–C-4–O-1′–C-1′,

$\phi^{H}_{2\rightarrow1}$ by atoms H-1′–C-1′–O-1′–C-4, $\psi^{H}_{2\rightarrow1}$, by atoms H-4–C-4–O-1′–C-1′,

$\phi_{3\rightarrow2}$ by atoms O-5″–C-1″–O-1″–C-4′, $\psi_{3\rightarrow2}$, by atoms C-5′–C-4′–O-1″–C-1″,

$\phi^{H}_{3\rightarrow2}$ by atoms H-1″–C-1″–O-1″–C-4′, and $\psi^{H}_{3\rightarrow2}$, by atoms H-4′–C-4′–O-1″–C-1″.

The orientation of the hydroxyl hydrogen atoms is indicated by χ_n, defined by the atoms H-*n*–C-*n*–O-*n*–H(O)-*n*, while χ_6 is defined by the atoms C-5–C-6–O-6–H(O)-6, and ω by the atoms O-5–C-5–C-6–O-6, singly- or doubleprimed when necessary. Their values are described by a one-letter code:[31] **S** for angles between -30 and $+30°$, **g** for 30–80°, **T** for angles with absolute value larger than 150°, and **G** for angles between -30 and $-80°$. Free energies were calculated from the vibrational analysis of the minima, with no special treatment for the low-frequency vibrations:[32] i.e., the effect of frequencies equal or lower than 20 cm^{-1} was added to the MM3 output values of vibrational enthalpies and entropies. Coordinates of crystalline compounds studied by X-ray diffraction were obtained from the Cambridge Structural Database.[33,34]

2.1. Generation of disaccharide maps

The maps were generated following the general procedure already described.[35,36] The starting orientations of the secondary hydroxyl and hydroxymethyl groups were taken from those yielding at least one grid point in the 8 kcal map reported by Dowd and co-workers[11,12] From these orientations (six for β-cellobiose[12] and 11 for α-maltose[11]), low-energy conformers were generated in different regions of the ϕ, ψ space, varying also the primary hydroxyl torsion angles. These conformers were the starting points for the generation of the maps. For β-cellobiose, 28 different conformers were used, corresponding to 16 unique exocyclic angle orientations. For α-maltose, 45 different minima were utilized, with 26 unique orientations of exocyclic angles. To generate the maps, the angles ϕ and ψ were varied using a 20° grid, using the dihedral driver 2 (sequential) for all the conformers, and the dihedral driver 4 (from the initial structure) for each of the unique orientation of exocyclic angles. The angle ψ was varied fully (0–340°), while ϕ was varied in the low-energy region (160–360° for β-cellobiose, and 20–200° for α-maltose), according to the published data.[11,12] At each point, energies were calculated after minimization with restraints for these two angles, but allowing the other variables to relax. The optimization was terminated when the decrease in energy converged to a value lower than 2 cal/mol. By recording only the lowest energy values for each ϕ, ψ combination, conformational adiabatic maps, or energy surfaces as function of ϕ and ψ angles were produced. For cellobiose, a separate calculation for the side-of-the-map minimum-energy region[13] was carried out using nine starting structures in that area.[12]

The same starting points and procedure were carried out to produce the 2D plots: in those cases, only the ψ angle was restrained, and the 2D conformational adiabatic plots as function of the ψ angle were obtained.[27]

2.2. Generation of trisaccharide minima

Different starting orientations of the hydroxyl and hydroxymethyl groups were tested using the conformers that yielded at least one low-energy grid point in the disaccharide maps: for the reducing and non-reducing ends (monosaccharides I and III), the orientations obtained for the reducing and non-reducing ends of the equivalent disaccharides were used, respectively. For monosaccharide II, both the orientations occurring at the reducing and non-reducing end of the disaccharide were used. In this way, for β-cellotriose, 256 different orientations of the exocyclic groups were tested (8 for monosaccharide I, 8 for monosaccharide II, and 4 for monosaccharide III), while for α-maltotriose, 324 different orientations appeared ($4 \times 9 \times 9$). In an auto-

mated fashion, unrestrained MM3 full-matrix calculations were carried out for points starting at each of those orientations, each one at a different combination of the ϕ, ψ angles (in either of both linkages) which gives rise to a minimum in the disaccharide maps (three for cellobiose and four for maltose). Thus, for cellotriose, 2304 structures were tested ($256 \times 3 \times 3$), while for maltotriose, 5184 structures were tested ($256 \times 4 \times 4$). The output was cleaned up for repetitions, structures with negative or zero eigenvalues, etc., and finally for each minimum, only those orientations with an energy up to 1 kcal above the lowest in that $\psi_{2\rightarrow1}, \psi_{3\rightarrow2}$ region (or higher than that value, but with a very low free energy) were left. In this way, for β-cellotriose, 144 different conformers were found, corresponding to 68 unique orientations of the exocyclic groups. On the other hand, for α-maltotriose, 259 different conformers were generated, related to 157 unique orientations of the exocyclic groups.

2.3. Generation of trisaccharide maps

The maps were generated as already described for the disaccharides. Both the dihedral drivers 2 and 4 were used: the first one for all the conformers, and the second one for each unique orientation of exocyclic angles. The angles $\psi_{2\rightarrow1}$ and $\psi_{3\rightarrow2}$ were fully varied using a 20° grid. At each point, energies were calculated after minimization with restraints for these two angles but allowing the other variables to relax. The optimization was terminated when the decrease in energy converged to a value lower than 2 cal/mol. The conformational adiabatic maps, or energy surfaces as function of both ψ angles were produced. In order to recalculate the surface in the region where the main minima appear (both ψ between ca. 170 and 270°), the starting points that yielded low-energy grid points in this region (73 minima related to 44 unique conformations for cellotriose, 65 minima related to 44 unique conformations for maltotriose) were submitted to calculations using the same procedure described above, but with a 5° grid.

2.4. Flexibility measurements

The absolute flexibilities for di- and trisaccharides were calculated as described previously.[25,36,37] First, the energies and geometries of the transition states between minimum energy regions were calculated: they were first estimated from the walk within the adiabatic maps, and then determined by a full-matrix analysis, confirming that only one negative eigenvalue appeared. When more than one transition state was present in the same region that with lower energy was considered. Then, the absolute flexibility Φ was calculated as:

$$\Phi_{p\theta_l} = \sum_{i=1}^{n} \left(\frac{e^{-E_i/RT}}{\sum_{k=1}^{n} e^{-E_k/RT}} \right) \times \left[\sum_{j=1}^{m} (e^{-(E_j - E_{gm})/RT}) \times \left(\frac{\sum_{l=1}^{P} |\theta_{l,i} - \theta_{l,j}|}{p \times 360°} \right) \right]$$

where E_{gm} is the energy of the global minimum, n is the number of minima (indexes i and k), m the number of transition states (index j) surrounding minimum i, p is the number of dihedral angles θ been monitored (index l), measured in degrees, R is the universal gas constant, and T the temperature (set to 25 °C = 298.16 K). The above-mentioned formula was also utilized to calculate the absolute flexibilities of the trisaccharides with respect to each glycosidic linkage. For this purpose, the absolute flexibility for each of the paths involving a neat variation of the ψ angle corresponding to this linkage was calculated independently. For each ψ angle all these flexibilities, weighed through their Boltzmann populations were added.

The partition functions were calculated as:[36]

$$q_{p\theta_l} = \prod_{l=1}^{p} \Delta\theta_l \times \sum_{i=1}^{ES} e^{-(E_i - E_{gm})/RT}$$

where $\Delta\theta$ are the grid spacings (20° for full maps, 5° for amplifications) and the summation is carried out over the entire surface determined (e.g., ES = 324 for full maps). French and co-workers[38] used the name 'probability volume' for this function. The partial flexibility on each of the ψ torsional angles of the trisaccharides, was evaluated by generating estimates of the adiabatic [energy vs. $\psi_{3\rightarrow2}$] and [energy vs. $\psi_{2\rightarrow1}$] relationships. These were created by recording the minimum energy in the amplified maps (5° grid) for each column and for each row of data, respectively. From these data, partial $q_{\psi_{3\rightarrow2}}$ and $q_{\psi_{2\rightarrow1}}$ values were calculated using the above-mentioned equation, which were extended to the whole ψ range by adding the effect of the remainder of the map (20° grid).

3. Results

The MM3 adiabatic conformational surfaces for β-cellobiose and α-maltose, depicted as contour maps are shown on Fig. 1. Only the main ϕ section was taken into account in the plot, disregarding side-of-the-map minima[13] (see below). Table 1 shows the geometrical and energy characteristics of the lower-energy minima in each region.

Fig. 2 shows the energy plot for both disaccharides, but related just to the glycosidic angle ψ.[27] The small geometrical differences between the minima, as well as the low-energy barriers preclude observing neat minima in the **A**–**B** regions. However, the comparison is clear:

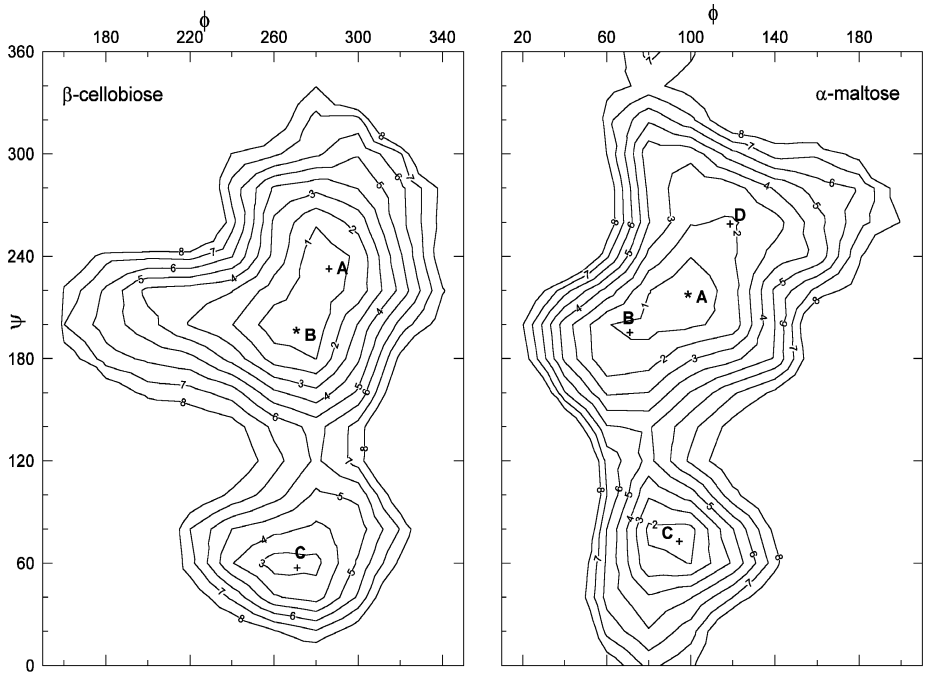

Fig. 1. MM3(92) adiabatic conformational maps of β-cellobiose and α-maltose at $\varepsilon = 4$. Iso-energy contour lines are graduated in 1 kcal/mol increments above the global minimum. The symbols indicate: (*) MM3 global minima; (+) MM3 local minima.

Table 1
Torsion angles (°), relative steric and free energies (kcal/mol) and exocyclic angles for the minimum-energy conformations [a] obtained for β-cellobiose and α-maltose using the MM3 force-field. Selected data for the main transition states (TS) is also included

	ϕ, ψ	ϕ_H, ψ_H	E_{rel}	G_{rel}	Exocyclic torsion angles [b]			
					$\chi_{2'}\chi_{3'}\chi_4$	$\omega'\chi_{6'}$	$\chi_1\chi_2\chi_3$	$\omega\chi_6$
β-Cellobiose								
A	286, 234	47, −5	0.10		GgG	gG	GgG	gG
	283, 231	45, −9		0.17	GgG	gT	GgG	gG
B	270, 197	32, −45	0.00	0.00	GgG	gT	GgG	gG
C	269, 56	31, 174	2.22		GgG	gG	gGg	gG
	270, 56	32, 174		3.39	GgG	gG	gGg	gT
TS **A**↔**B**	278, 218	40, −23	0.31					
α-Maltose								
A	99, 217	−21, −23	0.00		gGS	gG	ggG	Gg
	98, 217	−21, −23		0.00	gSG	gG	ggG	Gg
B	68, 193	−53, −49	0.58		TgG	gG	GTg	gG
	69, 193	−52, −48		0.42	GgG	gG	ggg	gG
C	92, 74	−28, −169	0.97	1.98	GgG	gT	ggG	gG
D [c]	120, 261	1, 25	1.90		GgG	gG	ggG	Gg
	118, 259	−1, 22		1.64	GgG	gG	ggG	gG
TS **A**↔**B**	77, 200	−44, −41	0.63					
TS **A**↔**D**	113, 247	−6, 10	2.05					

[a] When the steric energy minimum and the free energy minimum structures are not the same, the first line shows the data corresponding to the strain energy minimum, and the second line the data corresponding to the free energy minimum.
[b] For nomenclature, see Section 2.
[c] Another minimum at $\phi, \psi = 101, 279°$ appears only for a given combination of exocyclic chain angles.

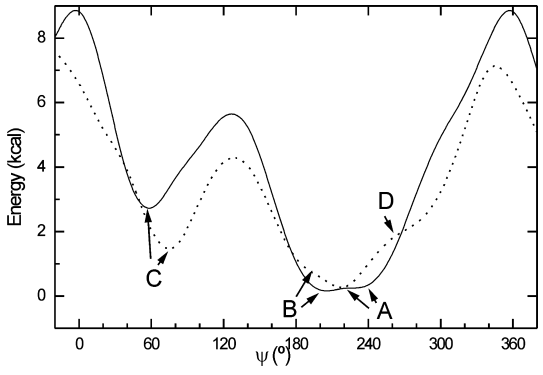

Fig. 2. MM3(92) relaxed surface (2D plot) for β-cellobiose (solid) and α-maltose (dashed) at $\varepsilon = 4$. Position of the minima is shown in both plots.

the **A**–**B** region well is wider for cellobiose, while the **C** region carries less energy for maltose.

The MM3 PES of β-cellotriose determined as a contour map relating the energy with both ψ glycosidic angles is shown in Fig. 3, while the plot obtained by recalculation in the region **A**–**B** of low-energy ($\psi_{3\to2}$ from 170 to 265°, $\psi_{2\to1}$ from 170 to 270°) is shown on Fig. 4. Table 2 indicates the geometrical and energy data on the minima obtained in each region. The minima are named by a two-letter code according to the minimum energy region (**A**, **B** or **C**) of the $3\to2$ linkage (first letter) and the $2\to1$ linkage (second letter). The equivalent maps and data for α-maltotriose are shown on Figs. 5 and 6, and Table 3, respectively. In this case, the map was recalculated in the region of $\psi_{3\to2}$ from 170 to 285° and $\psi_{2\to1}$ from 170 to 270°. It should be mentioned that the surface of maltotriose is very complex, as in the generation of the minima many calculations yielded negative or zero eigenvalues. The location of the minima finally determined was often very sensitive to the exocyclic chains orientations. Thus, sometimes shifts of ϕ and ψ angles within the **A**, **B** and **D** regions were observed. In special combinations of exocyclic chains, minima further away from region **D** appeared for the linkage $3\to2$. They were labeled as **EA** and **EB**. Such complexity of the PES under different methods was already mentioned for maltose.[20] It should be mentioned that although minima in any of the **D** regions are true minima, they are usually not part of the adiabatic map, i.e., there are points (not minima) with the same ψ angles, but lower energies, as already mentioned elsewhere.[13] As expected, considering the similar conformational behavior of both linkages for each trisaccharide, substantial diagonal symmetry is observed in the maps. Table 4 shows the flexibility measurements carried out using the data obtained for

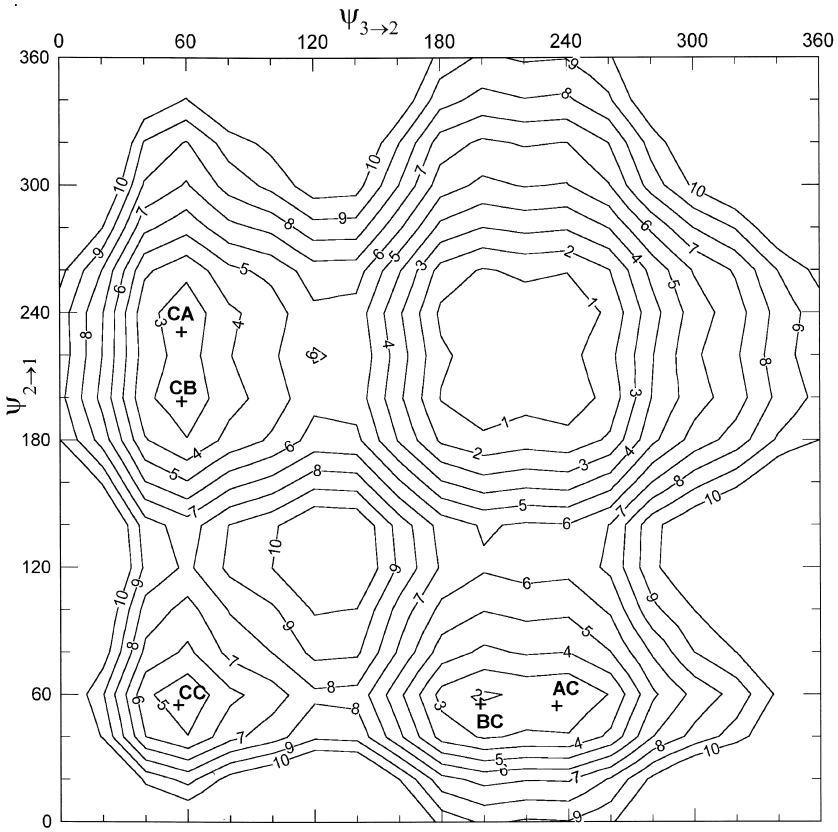

Fig. 3. MM3(92) adiabatic conformational map of β-cellotriose (energy vs. $\psi_{3\to2}$, $\psi_{2\to1}$) at $\varepsilon = 4$. Iso-energy contour lines are graduated in 1 kcal/mol increments above the global minimum. The symbol (+) indicates some of the MM3 local minima.

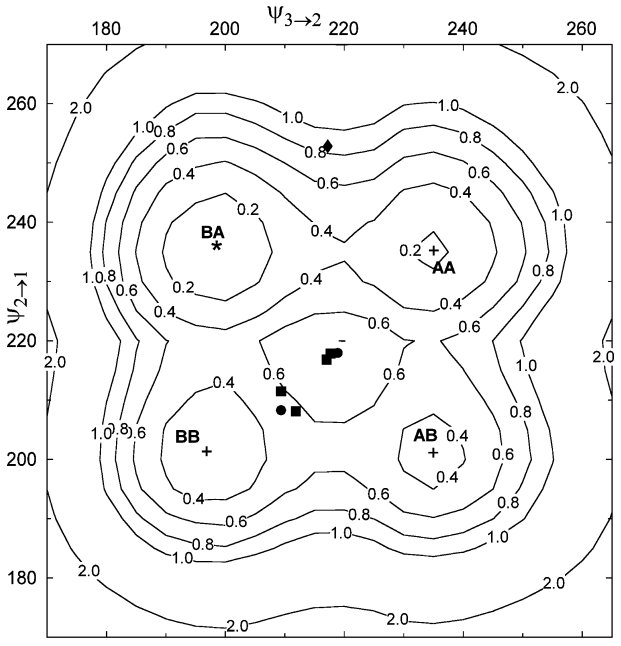

Fig. 4. MM3(92) adiabatic conformational map of β-cellotriose recalculated in a low-energy region. Iso-energy contour lines are graduated in 0.2 kcal/mol increments above the global minimum, up to 1 kcal/mol. The symbols indicate: (*) MM3 global minima; (+) MM3 local minima; reported crystal structures for: (●) different monomeric units of methyl β-cellotrioside ethanolate/hydrate,[39] (◆), β-cellotriose undecaacetate,[40] and (■) β-cellotetraose hemihydrate[41] (consecutive cellotriose units in each monomeric unit).

the di- and trisaccharides under study. For β-cellobiose, the contribution of the minimum with a ϕ angle shifted in ca. 120° (side-of-the-map[13]) to the total flexibility was only 0.04%, thus justifying disregarding this minimum. Table 5 shows the main hydrogen bond arrangements established for both trisaccharides in each minimum.

4. Discussion

The conformational characteristics of maltose and cellobiose were the subject of most of the earlier molecular modeling studies[3–21] devoted to disaccharides. Using MM3, a force-field with good parameterization for carbohydrates, Dowd and co-workers obtained the adiabatic conformational surfaces of both anomeric forms of both disaccharides (as well as those from other α- and β-linked disaccharides)[11,12] at a dielectric constant of 4. Further work[3,13] was made with improved versions of MM3 using different dielectric constants. The use of an $\varepsilon = 3$ for maltose was suggested.[3]

For β-cellobiose, the map currently obtained (Fig. 1) using MM3(92) is very similar to those obtained previously at similar dielectric constants[3,12,13] although the geometry of the minima is slightly shifted. The energy difference between minima **A** and **B** appears to be very small (Table 1, Fig. 2). While for β-cellobiose, the crystal structure carries its ϕ, ψ angles in the **A** region,[44,45] for the methyl β-cellobioside methanolate the conformations fall very close to our **B** minimum.[5,46] Crystal data for other cellobiose derivatives appear throughout the entire **A**–**B** region.[3,12,47] Rees[13] assumed that the solution conformation of cellobiose was the same as that obtained for the crystal (between the **A** and **B** minima, but closer to the **A** minimum). However, further attempts to determine the conformation of cellobiose and derivatives in solution using optical rotation, NOE and coupling constant measurements[15,16,18] indicated a flat potential surface in the **A**–**B** region, with populations of **A** and **B** conformers approximately equal,[15,18] and only small proportions of conformers in other regions. It was shown[48] that the hydrogen bonds present in the crystal (between H(O)-3 and O-5′) are disrupted in aqueous solution. The map shows the usual characteristics present in many disaccharides:[35,36] a low-energy **A**–**B** region with small energy differences and barriers, and another region (**C**) with slightly higher energy, but separated by a considerable barrier (Fig. 2) from the main region. Most of the conformers yielding low-energy minima in the adiabatic map carried both hydroxymethyl groups in *GT* orientation, as occurred in previous calculations and crystal structures.[12] Only seldom the non-reducing unit carried the *GG* orientation.

For α-maltose, the map (Fig. 1, Table 1) is also similar to those obtained previously[3,11,13] with different versions of MM3 and dielectric constants. Herein, four minima in the main area are observed. The minimum called **D** ('central'[13]) was first detected for β-maltose[11] but not for α-maltose. A recent work, however, detected this minimum for α-maltose, but failed to find minimum **B** at a similar dielectric constant.[13] Furthermore, the 'central' (**D**) minimum was found to carry an energy higher than that found for points in the adiabatic map with the same ϕ, ψ values.[13] The PES of α-maltose is more complex[20] than that of cellobiose, as different orientations of the exocyclic groups had some of their minima shifted to different ϕ, ψ angles. Minimum **A** was found to be the most stable (Table 1), closely followed by minimum **B**. Although minima in the **C** and **D** regions appear to be less favorable, the **C** minimum carries a surprisingly low energy (Table 1). However, as usually happens[36,49,50] the region **C** appears less favored when free energy calculations are performed. Crystal structures for maltose and derivatives appear mostly around minimum **A**, mostly towards the **D** region (the region between **A** and **D** was predicted as that most stable by DFT/ab initio calculations[20]), and only rarely reaching the **B** region.[3] On the other hand, experimental determinations in solution[15,17–19] indicate that probably region **B** is the

most populated in aqueous solution (the hydrogen-bond linking O-2′ and O-3 is broken[18]), closely followed by region **A**, being negligible the proportions of other conformations. This fact occurs in spite of the calculation of solvation effects, which led to **C** as the lowest energy region.[51] The conformational preference of maltose (within the region **A**–**B**) was found to be very sensitive to the solvent[15] and the anomeric status of the reducing end,[18] given the hydrogen bonding possibilities of the molecule. Most of the conformers yielding low-energy minima in the adiabatic map carried both hydroxymethyl groups in *GT* orientation, as occurred in previous calculations.[11] Only few of either of those units carried *GG* orientation. A crystal structure reported for β-maltose indicated a *GG* orientation for the reducing unit and a *GT* orientation for the non-reducing unit.[52] The four-minima pattern found here is very similar to that obtained by Tran and co-workers using a rigid-residue analysis.[9]

Partition function and absolute flexibility measurements (Table 4) indicate that the β-cellobiose glycosidic linkage is more flexible than that of α-maltose. This has already been predicted,[10,13] and agrees with the expected increase in flexibility arising from a diequatorial linkage against an axial–equatorial one.[36,38,50] The expression of the flexibility upon different angles (Table 4) is clearly showing that the increased flexibility of cellobiose is gained in the ψ direction. Within the ϕ coordinate, certainly maltose should be considered somehow more flexible than cellobiose, as its map (Fig. 1, Table 1) is showing a 50° span of ϕ between minima **B** and **D**, almost three times larger than that encountered for cellobiose.

Conformational analysis of tri- or higher oligosaccharides has been usually carried out by NMR techniques.[23,53] Molecular modeling has also been used, sometimes using molecular dynamics,[22] other heuristic procedures,[25] or partial rigid-residue analysis[24,54] in order to explore the whole conformational space. When all the glycosidic linkages were studied, each one was taken independently, giving rise to one ϕ, ψ contour map per glycosidic linkage.[22–26] Mazeau and Pérez[26] have determined the adiabatic maps of 18 disaccharides which act as building blocks of rhamnogalacturonan II, and later calculated the possible conformations of the oligosaccharides generated with them, projecting the

Table 2
Torsion angles (°), relative steric and free energies (kcal/mol) and exocyclic angles for the minimum-energy conformations obtained for β-cellotriose using the MM3 force-field. Selected data for the main transition states (TS) is also included

	$\phi_{3\to2}$, $\psi_{3\to2}$	(ϕ^H, ψ^H)	$\phi_{2\to1}$, $\psi_{2\to1}$	(ϕ^H, ψ^H)	E_{rel} [a]	Exocyclic torsion angles [b]		
Steric energy minima								
AA	286, 234	47, −5	284, 235	46, −4	0.16	GgGgG	gGgG	GgGgG
AB	286, 235	47, −5	268, 201	30, −40	0.26	GgGgG	gGgT	GgGgG
AC	285, 234	47, −5	269, 55	30, 174	1.86	GgGgG	gGgG	GgGgG
BA	270, 197	32, −45	284, 235	46, −4	0.00	GgGgT	gGgG	GgGgG
BB	270, 196	32, −46	268, 201	30, −41	0.21	GgGgT	gGgT	GgGgG
BC	270, 197	32, −45	268, 55	30, 174	1.73	GgGgT	gGgG	GgGgG
CA	270, 55	32, 174	285, 233	47, −6	2.13	GgGgG	GggG	GgGgG
CB	270, 56	32, 175	270, 198	32, −44	2.21	GgGgG	GggT	GgGgG
CC	271, 55	33, 173	269, 54	31, 173	3.94	GgGgG	GggG	gGggG
Free energy minima								
AA	284, 231	46, −8	281, 230	43, −9	0.47	GgGgT	gGgT	GgGgG
AB	281, 230	42, −10	268, 201	30, −41	0.18	gGSgT	gGgT	GgGgG
AC	283, 231	45, −9	269, 55	30, 174	3.36	GgGgT	gGgG	GgGgG
BA	269, 201	30, −41	281, 230	43, −10	0.00	gGSgT	gGgT	GgGgG
BB	same as steric minimum				0.21	GgGgT	GGgT	GgGgG
BC	same as steric minimum				3.21	GgGgT	GGgG	GgGgG
CA	268, 59	30, 177	283, 231	45, −8	3.67	GgGgT	GggT	GgGgG
CB	267, 58	29, 177	270, 197	32, −45	3.49	GgGgT	GggT	GgGgG
CC	same as steric minimum				6.64	GgGgG	GggG	gGggG
Main transition states								
AA↔AB	286, 234	47, −5	276, 222	38, −19	0.52			
AA↔BA	278, 218	40, −23	284, 235	46, −4	0.41			
AB↔BB	277, 217	39, −24	268, 202	30, −40	0.52			
BA↔BB	270, 196	32, −45	277, 222	39, −19	0.55			

[a] Steric energy or free energy, depending on the listing.
[b] The angles are given in the order $\chi_{2''}\chi_{3''}\chi_{4''}$ $\omega''\chi_{6''}$ $\chi_{2'}\chi_{3'}$ $\omega'\chi_{6'}$ $\chi_1\chi_2\chi_3$ $\omega\chi_6$. For nomenclature of the angles, see Section 2.

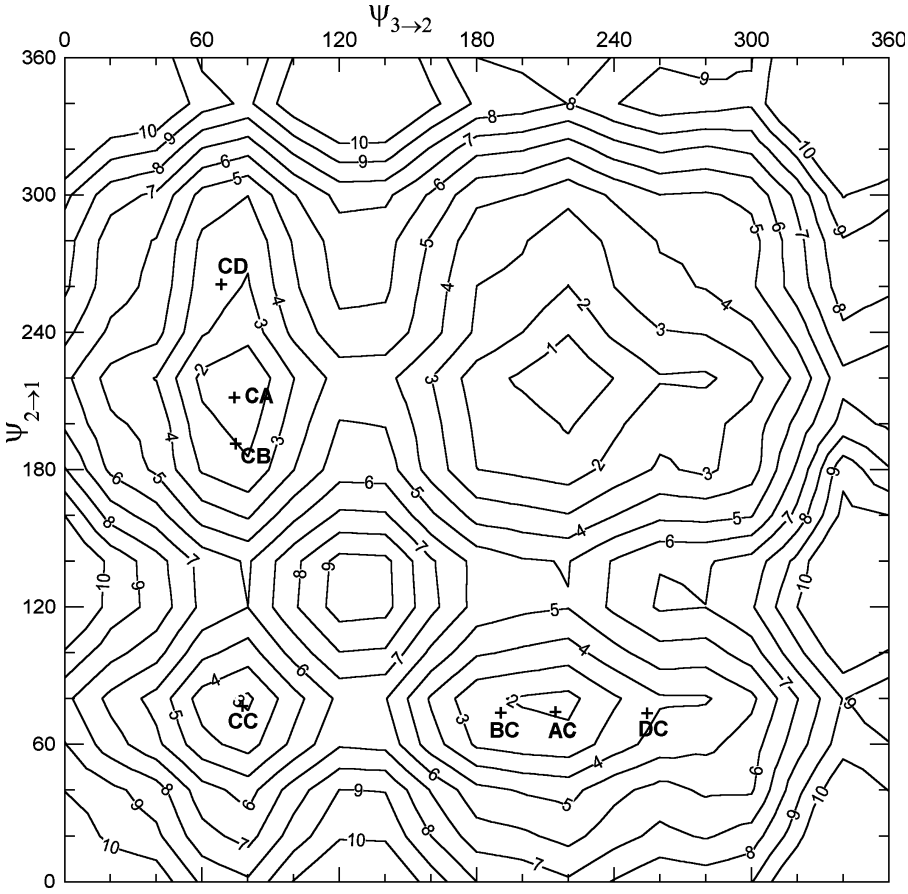

Fig. 5. MM3(92) adiabatic conformational map of α-maltotriose (energy vs. $\psi_{3\rightarrow2}$, $\psi_{2\rightarrow1}$) at $\varepsilon = 4$. Iso-energy contour lines are graduated in 1 kcal/mol increments above the global minimum. The symbol (+) indicates some of the MM3 local minima.

position of the minima obtained onto the disaccharides maps. However, they did not show a graphical relationship of the effect of one glycosidic linkage on another glycosidic linkage. With the usual representations of disaccharides adiabatic map as 3D contour plots (i.e., relating the energy with the glycosidic angles ϕ and ψ), representing a trisaccharide would require the use of a five-dimensional plot, beyond the possibility of human understanding. However, the ϕ glycosidic angle was found to take a more or less fixed value for most of the disaccharides, at least using MM3.[11–13] Even if the 'side-of-the-map' minima may be significant for some equatorially linked disaccharides,[13,27] their populations are usually negligible[13] when calculating at dielectric constants above 1.5. Furthermore, this minimum only accounts to 0.04% of the total population of β-cellobiose in the present work. Thus, it may be considered that there is no need to relate the glycosidic linkage features with angle ϕ. It was previously shown that the ϕ angle could also be allowed to relax, considering that a clear correlation was found between the 3D contour maps (energy vs. ϕ and ψ) and the 2D plots (energy vs. ψ).[27] Therefore, it is possible to represent the PES of a trisaccharide as a contour map, in which the energy is plotted against both ψ angles, while the ϕ angles are allowed to relax.

From the geometrical standpoint, the adiabatic map of β-cellotriose (Figs. 3 and 4) represents the crossing of the maps of each linkage behaving independently. Thus, the three minima appearing for each linkage are transformed into nine minima, with ϕ, ψ angles very close to those encountered for the disaccharide (cf. Tables 2 and 3). An almost square region with an energy below 1 kcal appears, encompassing a region with both ψ angles varying between 180 and 260° (-180 to -100°), and comprising the four main minima (**AA**, **AB**, **BA** and **BB**). The energy differences between these minima (Table 2) are not significant. About 2 kcal above the global minimum, the four minima carrying one angle in the **C** region and another in the **A** or **B** region appear (Table 2). These minima generate two oval minima regions with energies below 3 kcal (Fig. 3). The ninth minimum (**CC**) appears with even higher energy, as expected. Some maxima are also observed, for example those around $\psi, \psi = 120°$, 120° (Fig. 3), and 220°, 210° (Fig. 4). They are not transition states, as they carry more than one negative eigenvalue. A careful analysis of the energies involved in each

minimum is showing that, though the geometrical features of each linkage appear to be almost independent, the energies do not show the same behavior. The four minima in the **A**–**B** region have very similar energies (Table 2). However, **B** was the global minimum for cellobiose, while **BB** is not the global minimum for cellotriose: **BA** is the main minimum, and **AA** carries actually less energy than **BB**. In any case, the differences are very small, and even the four transition states have energies below RT (Table 2). The minima comprising one linkage in the **C** region of cellotriose have less relative energies than the **C** minimum in cellobiose (Tables 1 and 2). Furthermore, the presence of a **C** minimum in the $2\rightarrow1$ linkage (minima **AC** and **BC**) appears more favorable than that on the $3\rightarrow2$ linkage (minima **CA** and **CB**). All of the minima obtained using steric or free energy measurements carry all their hydroxymethyl groups in *GT* orientation (Table 2). However, in the adiabatic map, some of the grid points are originated in structures carrying at most one *GG* orientation (usually for monosaccharide I). Crystallographic studies on methyl β-cellotrioside ethanolate/hydrate[39] showed four independent molecules in the unit, arranged in an antiparallel fashion: two molecules showed both ψ angles around 208°, while the other two carried those angles at 218° (their ϕ values were between 263 and 269°), i.e., one pair close to the **BB** minimum, and the other pair in the middle of the four (Fig. 3). The ψ angles in both linkages of the same molecule are similar. An analogous result has been found for the two antiparallel monomers of the hydrate of β-cellotetraose[41] (Fig. 4). High quality difraction studies on cellulose II[55] and cellulose Iβ[56] also indicate similar ψ angles (around 215°). The studies on the oligosaccharides found all the hydroxymethyl groups in *GT* orientation,[39,41] as occurred with most of those found on cellulose II.[55] However, in cellulose Iβ the hydroxymethyl groups were found in *TG* orientation.[56] In the present work, *TG* orientation was not searched for, as modeling on cellobiose found this orientation not favorable.[12] On the other hand, a crystallographic study on the undecaacetate of β-cellotriose[40] showed different torsional angles for each glycosidic linkage: for $3\rightarrow2$, ϕ, ψ were equal to 262°, 217°, while for the $2\rightarrow1$ linkage, ϕ, ψ were 285°, 263°. Those values are not far from the **BA** minimum, herein found as the global one. Only the downstream end appeared in *GT* orientation, while the other two units carried *GG* orientations.[40] Hydrogen-bonding of the hydrogen linked to O-3 of one unit and O-5 of the neighboring unit appears (Table 5) for all the monosaccharide pairs in the **A** or **B** regions, since their energies very alike (only slightly higher for the **B** region). This interresidue hydrogen bond has already been observed.[48] When the glycosidic linkage orientation is that corresponding to the **C** minimum, the above mentioned-hydrogen bond is precluded, and replaced by another one between the primary alcohol hydrogen of one unit and O-6 of the neighboring unit.

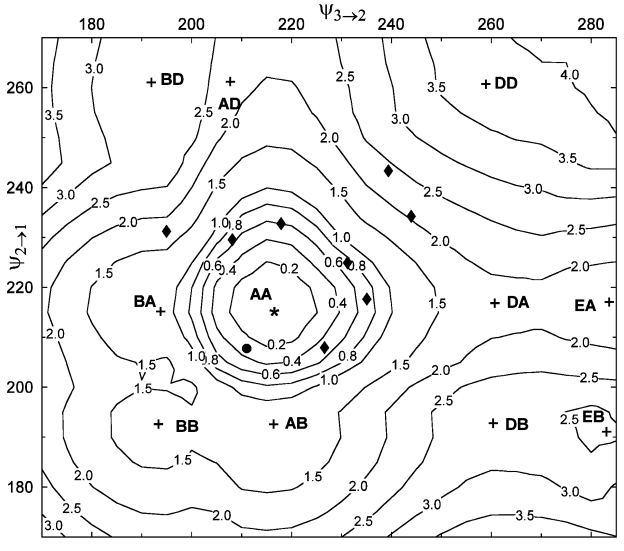

Fig. 6. MM3(92) adiabatic conformational map of α-maltotriose recalculated in a low-energy region. Iso-energy contour lines are graduated in 0.2 kcal/mol increments above the global minimum, up to 1 kcal/mol, and then in 0.5 kcal/mol increments. The symbols indicate: (*) MM3 global minima; (+) MM3 local minima; reported crystal structures for (●) methyl β-maltotrioside hydrate,[42] and (◆) barium bis(*p*-nitrophenyl)-α-maltohexaoside bis(triiodide) hydrate[43] (consecutive maltotriose units in each monomer).

In the equivalent adiabatic map of α-maltotriose (Figs. 5 and 6), the map shows again that each linkage behaves more or less independently. Thus, the four or five minima appearing for each linkage are converted into about 18 minima, with ϕ, ψ angles very close to those encountered for the disaccharide (cf. Tables 2 and 4). As a difference with the map of cellotriose, the region with an energy below 1 kcal is quite small and with a round shape, encircling only the global minimum (**AA**). Other low-energy minima (**AB**, **BA** and **BB**) appear in flatter surfaces, while those comprising a **D** minimum (**AD**, **BD**, **DA**, **DB** or **DD**) are not discernible by the contour, as expected, considering that they are not part of the adiabatic surface (see Section 3). About 2 kcal above the global minimum, the minima carrying one angle in the **C** region and the other in the **A** region appear (Table 3, Fig. 5), while those combining a **C** minimum with a **B** or a **D** minimum are hard to detect by the contour. At last, a small 3-kcal region containing the **CC** minimum appears. The maximum around $\psi, \psi = 120, 120°$ (Fig. 4) carries lower energy than for cellotriose. Although the low-energy region for maltotriose is smaller than for cellotriose, the total surface covered by the 10 kcal map is larger. The **AA** minimum in maltotriose appears more stable than the **A** minimum in maltose (cf. Tables 1 and 3). The **CA** minimum is particularly stable (Table 3). The **C** region appears more favorable on the $3\rightarrow2$ linkage than on the $2\rightarrow1$

Table 3
Torsion angles (°), relative steric and free energies (kcal/mol) and exocyclic angles for the minimum-energy conformations [a] obtained for α-maltotriose using the MM3 force-field. Selected data for the main transition states (TS) is also included

	$\phi_{3\to2}$, $\psi_{3\to2}$	(ϕ^H, ψ^H)	$\phi_{2\to1}$,$\psi_{2\to1}$	(ϕ^H, ψ^H)	E_{rel} [b]	Exocyclic torsion angles [c]		
Steric energy minima								
AA	99, 216	−20, −23	101, 216	−18, −24	0.00	gGSgG	gGGg	ggGgG
AB	102, 216	−18, −24	68, 192	−53, −50	1.10	gGgGg	gGgG	GTggG
AC	102, 214	−17, −26	92, 74	−28, −169	1.42	gGSgG	gGgT	ggGgG
AD	94, 208	−25, −33	121, 261	1, 25	2.69	GgGgG	GggG	ggGGg
BA	68, 193	−53, −48	99, 216	−20, −23	1.07	TgGgG	gSgG	ggGGg
BB	69, 193	−53, −49	68, 192	−54, −50	1.30	TgGgG	TggG	GTggG
BC	70, 194	−52, −48	92, 74	−28, −169	1.64 (2.36)	TgGgG	GggT	ggGgG
BD	68, 192	−54, −50	121, 261	1, 25	2.68	TgGgG	GggG	ggGGg
CA	92, 74	−28, −169	103, 213	−17, −27	0.75	GgGgT	gGgG	ggGgG
CB	92, 75	−28, −168	70, 192	−51, −49	1.72 (2.59)	GgGgT	gGgG	GTggG
CC	92, 74	−29, −169	92, 74	−28, −169	2.93 (3.82)	GgGgT	gGgG	ggGgG
CD	89, 69	−31, −174	119, 258	0, 22	4.82	GgGgT	gGgG	GTggG
DA	117, 261	−2, 24	99, 217	−20, −23	1.91	GgGgG	gGgG	ggGGg
DB	121, 260	2, 23	67, 192	−54, −49	2.98	TgGgG	TggG	GTggG
DC	124, 257	6, 21	92, 74	−28, −169	3.64	TgGgG	GggT	ggGgG
DD	122, 259	3, 22	121, 261	2, 25	4.44	TgGgG	GggG	ggGGg
EA [d]	94, 283	−27, 47	97, 216	−23, −23	1.69 (1.94)	GgGgG	gGgG	ggGGg
EB [d]	94, 282	−27, 46	67, 191	−55, −51	2.37 (2.33)	GgGgG	gGgG	GTggG
Free energy minima								
AA	101, 215	−18, −25	102, 214	−18, −26	0.00	gSGgT	gGgT	ggGgG
AB	102, 214	−18, −26	70, 193	−51, −48	0.21	gSGgG	gGgT	ggSGg
AC	101, 214	−18, −26	92, 74	−28, −169	1.82	gSGgG	gGgT	ggGgG
AD	90, 206	−30, −35	120, 259	1, 22	1.94	gGSgT	GggG	ggGgG
BA	69, 193	−52, −48	101, 214	−18, −26	0.96	GgGgG	gSgT	ggGgG
BB	70, 193	−51, −48	68, 192	−54, −49	0.56	gGSgT	TggG	ggSgG
BD	69, 193	−52, −49	120, 260	1, 23	1.90	gGSgT	GggG	ggGgG
CA	93, 74	−27, −169	102, 214	−17, −26	1.89	GgGgT	gGgT	ggGgG
CD	90, 69	−31, −174	118, 257	−1, 20	4.50	gGSgG	GggG	ggGgG
DA	113, 262	−7, 26	102, 216	−17, −24	1.64	GgGgT	gGGg	ggGgG
DB	116, 258	−3, 22	68, 193	−53, −49	2.50	TgGgT	GggG	ggggG
DC	119, 255	0, 18	92, 74	−28, −169	3.70	GgGgG	gGgT	ggGgG
DD	120, 257	0, 21	120, 260	1, 23	3.98	TgGgT	GggG	ggGgG
Main transition states								
AA↔AB	102, 216	−17, −24	77, 199	−43, −42	1.39			
AA↔BA	75, 199	−46, −42	100, 216	−20, −23	1.08			
AB↔BB	79, 201	−41, −40	68, 192	−54, −49	1.35			
BA↔BB	69, 194	−52, −48	75, 198	−46, −43	1.37			
AA↔EA	113, 243	−7, 6	99, 217	−20, −23	2.10			
AC↔BC	77, 200	−43, −41	92, 74	−28, −169	1.69			
AB↔EB	112, 244	−7, 6	68, 191	−54, −51	3.10			
BA↔BD	68, 192	−53, −49	118, 252	−2, 15	2.89			

[a] Some other minima appeared between regions **A** and **D**. These minima were used to construct the contour map, but are not included in this Table.

[b] Steric energy or free energy, depending on the listing. When it corresponds to the same minimum, free energy appears in parentheses.

[c] The angles are given in the order $\chi_{2''}\chi_{3''}\chi_{4''}$ $\omega''\chi_{6''}$ $\chi_{2'}\chi_{3'}$ $\omega'\chi_{6'}$ $\chi_1\chi_2\chi_3$ $\omega\chi_6$. For nomenclature of the angles, see Section 2.

[d] Only one exocyclic angle arrangement was studied.

Table 4
Corrected partition functions q and absolute flexibilities Φ calculated for the compounds under study

	$q_{\phi,\psi}$ (deg^2)	q_{ψ} (°)	$q_{\phi,\psi}/q_{\psi}$ (°)	$\Phi_{\phi,\psi}$ ($\times 10^4$)	Φ_{ψ} ($\times 10^4$)	$\Phi_{\phi,\psi}/\Phi_{\psi}$
β-Cellobiose	1255	56	22.5	216	303	0.71
α-Maltose	1161	40	28.8	162	148	1.10
	$q_{\psi,\psi}$ (deg^2)	q_{ψ} (°)	$\Phi_{\phi,\psi,\phi,\psi}$ ($\times 10^4$)	$\Phi_{\psi,\psi}$ ($\times 10^4$)	Φ_{ψ} ($\times 10^4$)	$\Phi_{\phi,\psi,\phi,\psi}/\Phi_{\psi,\psi}$
β-Cellotriose	2656	$q_{\psi_{3\to2}} = 51$ [a] $q_{\psi_{2\to1}} = 49$ [a]	151	211	$\Phi_{\psi 3\to2} = 282$ $\Phi_{\psi 2\to1} = 206$	0.72
α-Maltotriose	1239	$q_{\psi_{3\to2}} = 37$ [a] $q_{\psi_{2\to1}} = 33$ [a]	52	45	$\Phi_{\psi 3\to2} = 91$ $\Phi_{\psi 2\to1} = 73$	1.17

[a] Estimated from the 3D map (see Section 2).

linkage (in contrast with cellotriose, see above). Most of the minima carry their hydroxymethyl groups in *GT* orientation, although some appear in *GG* orientation (Table 3). Within the adiabatic map, only some of the grid points are originated in structures carrying one or two *GG* orientations (usually for monosaccharide I, less for monosaccharide III). Crystallographic studies on methyl β-maltotrioside hydrate[42] indicated ϕ, ψ angles of 82, 211° for the linkage $3\to2$ and 83, 208° for linkage $2\to1$, very close to our **AA** region (Fig. 6). On a dimer of a maltohexaose derivative,[43] several different ψ values were encountered. When paired, they are mostly scattered around the **AA** minimum (Fig. 6). This dispersion suggests that the difficulties of modeling the minimum energy conformations of maltose and derivatives are not just related to incomplete parameterization of force-fields,[20] but also arise from true physical complexities. These studies found most of the hydroxymethyl groups in *GG* orientation,[42,43] and only one in *GT* orientation.[43] Hydrogen bonding of the hydrogen linked to O-3 of one unit and O-2 of the neighboring unit appears (Table 5) for the monosaccharide pairs in the **A** and **D** regions (for the latter, sometimes the donor and acceptor are inverted). When the glycosidic linkage orientation is that corresponding to the **B** or the **C** minimum, the above-mentioned hydrogen bonds are precluded. In the **C** region, they are replaced by another one between the same hydrogen (that linked to O-3 of one unit) and the O-6 of the neighboring unit, while for the **B** region no strong hydrogen bonds are found to occur.

Flexibility measurements for cellotriose and maltotriose (Table 4) follow the trend shown for the corresponding disaccharides: the β-linked trisaccharide is much more flexible than the α-linked one. Furthermore, the partition function measurements give enhanced differences, as expected. The parameter q_{ψ} for cellobiose is 40% larger than for maltose; if both ψ angles in the trisaccharide behave in an independent fashion, it should be expected that the $q_{\psi,\psi}$ of the trisaccharide should be equal to q_{ψ} of the disaccharide squared. The lower value obtained in both cases (Table 4) is indicating a decrease of the flexibilities of the individual trisaccharide linkages with respect to that of the disaccharide, possibly due to the presence of cooperative interactions. Another parameter that can help to confirm this decreased flexibility is an estimation of the partition function values for each individual linkage. The method of calculation of these parameters can lead to a small underestimation, as it is determined in grid points and not with the second angle fully relaxed (see Section 2). However, as it was calculated mostly on a 5° grid, the underestimation should indeed be small. These parameters also show a decrease in flexibility of a

Table 5
Hydrogen-bond arrangements (with $E_{HB} > 0.3$ kcal/mol) established for every MM3 minimum of cellotriose and maltotriose [a]

Hydrogen bond	Minima
β-Cellotriose	
H(O)-3′–O5″	**AA**, **AB**, **AC** (0.56–0.58), **BA**, **BB**, **BC** (0.60–0.63)
H(O)-3–O5′	**AA**, **BA**, **CA** (0.55–0.61), **AB**, **BB**, **CB** (0.65–0.68)
H(O)-6′–O6	**AC**, **BC**, **CC** (0.46–0.50)
H(O)-6″–O6′	**CA**, **CB**, **CC** (0.37–0.45)
α-Maltotriose	
H(O)-3′–O2″	**AA**, **AB**, **AC** (0.52–0.60), **DA** (0.33)
H(O)-3–O2′	**AA**, **BA**, **CA**, **DA** (0.51–0.63), **AD**, **BD**, **CD**, **DD** (0.31–0.38)
H(O)-2″–O3′	**DB**, **DC**, **DD** (0.57–0.62)
H(O)-3–O6′	**AC**, **BC**, **CC**, **DC** (0.51–0.63)
H(O)-3′–O6″	**CA**, **CB**, **CC** (0.52–0.55)

[a] In parentheses, energy involved in the hydrogen bond (in kcal/mol).

linkage when passing from a disaccharide to a trisaccharide, as shown by Mazeau and Pérez.[26] Furthermore, our results indicate that the 2→1 linkage (closer to the reducing end) is even less flexible than the 3→2 linkage. Similar results are obtained by the use of absolute flexibilities: the Φ_{ψ} parameter is reduced from a value of 303 in cellobiose to 282 for the 3→2 linkage and 206 for the other linkage of cellotriose. For the α-linked compounds the reduction is even larger, suggesting that they have higher restrictions: the 148 value for maltose is reduced to 91 and 73 in both linkages of maltotriose. As expected, the $\Phi_{\phi,\psi}/\Phi_{\psi}$ ratios for the disaccharides stay similar to the equivalent ratios in the trisaccharides, as no major geometrical changes are produced. The higher flexibility of the 3→2 linkage of maltotriose (with respect to the 2→1 linkage) occurs not only within the central region, but also extending to the minima comprising one linkage in the **C** region (Fig. 5). On the other hand, for cellotriose, the higher 'horizontal' flexibility occurs in the main **A**–**B** region, as Fig. 4 clearly shows, but the region comprising a **C** minimum for the 2→1 linkage appears favored. However, this factor does not compensate the higher flexibility of the 3→2 linkage in the most populated area.

This work shows that mapping of trisaccharides by the way of 3D contours is possible, and gives information on the conformations and their interconversions which is harder to view without the picture. Flexibility measurements may also help to recognize their conformational features. It may be expected that further work, for instance on products with possibly interacting linkages (as 1→2 linked trisaccharides), and/or two different linkages, will throw light on these subjects.

Acknowledgements

Both authors are Research Members of the National Research Council of Argentina (CONICET). This work was supported by grants from UBA (X087), Antorchas-Vitae, and CONICET.

References

1. French, A. D.; Brady, J. W. *ACS Symp. Ser.* **1990**, *430*, 1–19.
2. Engelsen, S. B.; Rasmussen, K. *Int. J. Biol. Macromol.* **1993**, *15*, 56–62.
3. French, A. D.; Dowd, M. K. *J. Mol. Struct. (Theochem.)* **1993**, *286*, 183–201.
4. Melberg, S.; Rasmussen, K. *Carbohydr. Res.* **1979**, *69*, 27–38.
5. Melberg, S.; Rasmussen, K. *Carbohydr. Res.* **1979**, *71*, 25–34.
6. Tvaroška, I.; Pérez, S. *Carbohydr. Res.* **1986**, *149*, 389–410.
7. French, A. D. *Biopolymers* **1988**, *27*, 1519–1523.
8. Ha, S. N.; Madsen, L. J.; Brady, J. W. *Biopolymers* **1988**, *27*, 1927–1952.
9. Tran, V.; Buléon, A.; Imberty, A.; Pérez, S. *Biopolymers* **1989**, *28*, 679–690.
10. French, A. D. *Carbohydr. Res.* **1989**, *188*, 206–211.
11. Dowd, M. K.; Zeng, J.; French, A. D.; Reilly, P. J. *Carbohydr. Res.* **1992**, *230*, 223–244.
12. Dowd, M. K.; French, A. D.; Reilly, P. J. *Carbohydr. Res.* **1992**, *233*, 15–34.
13. Mendonca, S.; Johnson, G. P.; French, A. D.; Laine, R. A. *J. Phys. Chem., Sect. A* **2002**, *106*, 4115–4124.
14. Rees, D. A. *J. Chem. Soc., Sect. B* **1970**, 877–884.
15. Lipkind, G. M.; Verovsky, V. E.; Kochetkov, N. K. *Carbohydr. Res.* **1984**, *133*, 1–13.
16. Lipkind, G. M.; Shashkov, A. S.; Kochetkov, N. K. *Carbohydr. Res.* **1985**, *141*, 191–197.
17. Shashkov, A. S.; Lipkind, G. M.; Kochetkov, N. K. *Carbohydr. Res.* **1986**, *147*, 175–182.
18. Stevens, E. S.; Sathyanarayana, B. K. *J. Am. Chem. Soc.* **1989**, *111*, 4149–4154.
19. Stevens, E. S. *Biopolymers* **1992**, *32*, 1571–1579.
20. Momany, F. A.; Willett, J. L. *J. Comput. Chem.* **2000**, *21*, 1204–1219.
21. Momany, F. A.; Willett, J. L. *Carbohydr. Res.* **2000**, *326*, 194–209.
22. Homans, S. W. *Biochemistry* **1990**, *29*, 9110–9118.
23. Homans, S. W.; Forster, M. *Glycobiology* **1992**, *2*, 143–151.
24. French, A. D.; Mouhous-Riou, N.; Pérez, S. *Carbohydr. Res.* **1993**, *247*, 51–62.
25. Koča, J.; Pérez, S.; Imberty, A. *J. Comput. Chem.* **1995**, *16*, 296–310.
26. Mazeau, K.; Pérez, S. *Carbohydr. Res.* **1998**, *311*, 203–217.
27. Stortz, C. A.; Cerezo, A. S. *Carbohydr. Res.* **2002**, *337*, 1861–1871.
28. Allinger, N. L.; Yuh, Y. H.; Lii, J.-H. *J. Am. Chem. Soc.* **1989**, *111*, 8551–8566.
29. Allinger, N. L.; Rahman, M.; Lii, J.-H. *J. Am. Chem. Soc.* **1990**, *112*, 8293–8307.
30. MM3 (96). *Bull. QCPE* **1997**, *17* (1), 3.
31. Engelsen, S. B.; Koča, J.; Braccini, I.; Hervé du Penhoat, C.; Pérez, S. *Carbohydr. Res.* **1995**, *276*, 1–29.
32. Engelsen, S. B.; Rasmussen, K. *J. Carbohydr. Chem.* **1997**, *16*, 773–788.
33. Allen, F. H.; Kennard, O. *Chem. Des. Autom. News* **1993**, *8*, 31–37.
34. Bruno, I. J.; Cole, J. C.; Lommerse, J. P. M.; Rowland, R. S.; Taylor, R.; Verdonk, M. L. *J. Comput.-Aided Mol. Des.* **1997**, *11*, 525–537.
35. Stortz, C. A. *Carbohydr. Res.* **1999**, *322*, 77–86.
36. Stortz, C. A. *Carbohydr. Res.* **2002**, *337*, 2311–2323.
37. Koča, J. *J. Mol. Struct.* **1993**, *291*, 255–269.
38. French, A. D.; Kelterer, A.-M.; Johnson, G. P.; Dowd, M. K.; Cramer, C. J. *J. Comput. Chem.* **2001**, *22*, 65–78.
39. Raymond, S.; Henrisat, B.; Qui, D. T.; Kvick, Å.; Chanzy, H. *Carbohydr. Res.* **1995**, *277*, 209–229.
40. Pérez, S.; Brisse, F. *Acta Crystallogr., Sect. B* **1977**, *33*, 2578–2584.
41. Pangborn, W.; Langs, D.; Pérez, S. *Int. J. Biol. Macromol.* **1985**, *7*, 363–369.
42. Gessler, K.; Krauss, N.; Steiner, T.; Betzel, C.; Sarko, A.; Saenger, W. *J. Am. Chem. Soc.* **1995**, *117*, 11397–11406.
43. Hinrichs, H.; Saenger, W. *J. Am. Chem. Soc.* **1990**, *112*, 2789–2796.
44. Brown, C. J. *J. Chem. Soc., Sect. A* **1966**, 927–932.
45. Chu, S. S. C.; Jeffrey, G. A. *Acta Crystallogr., Sect. B* **1968**, *24*, 830–838.

46. Ham, J. T.; Williams, D. G. *Acta Crystallogr., Sect. B* **1970**, *26*, 1373–1383.
47. Peralta-Inga, Z.; Johnson, G. P.; Dowd, M. K.; French, A. D.; Rendleman, J. A.; Stevens, E. D.; French, A. D. *Carbohydr. Res.* **2002**, *337*, 851–861.
48. Leeflang, B. R.; Vliegenthart, J. F. G.; Kroon-Batenburg, L. M. J.; van Eijck, B. P.; Kroon, J. *Carbohydr. Res.* **1992**, *230*, 41–61.
49. Stortz, C. A.; Cerezo, A. S. *J. Carbohydr. Chem.* **2000**, *19*, 1115–1130.
50. Stortz, C. A.; Cerezo, A. S. *J. Carbohydr. Chem.* **2002**, *21*, 355–371.
51. Tvaroška, I. *Biopolymers* **1982**, *21*, 1887–1897.
52. Quigley, G. J.; Sarko, A.; Marchessault, R. H. *J. Am. Chem. Soc.* **1970**, *92*, 5834–5839.
53. Poppe, L.; Dabrowski, J.; von der Lieth, C.-W.; Koike, K.; Ogawa, T. *Eur. J. Biochem.* **1990**, *189*, 313–325.
54. Li, J.; Ksebati, M. B.; Zhang, W.; Guo, Z.; Wang, J.; Yu, L.; Fang, J.; Wang, P. G. *Carbohydr. Res.* **1999**, *315*, 76–88.
55. Langan, P.; Nishiyama, Y.; Chanzy, H. *J. Am. Chem. Soc.* **1999**, *121*, 9940–9946.
56. Nishiyama, Y.; Langan, P.; Chanzy, H. *J. Am. Chem. Soc.* **2002**, *124*, 9074–9082.